Fluxes of nitrogen oxides over a temperate deciduous forest

Cassandra Volpe Horii, J. William Munger, and Steven C. Wofsy

Division of Engineering and Applied Sciences and Department of Earth and Planetary Science, Harvard University, Cambridge, Massachusetts, USA

Mark Zahniser, David Nelson, and J. Barry McManus

Aerodyne Research, Inc., Billerica, Massachusetts, USA

Received 4 November 2003; revised 13 February 2004; accepted 23 February 2004; published 23 April 2004.

[1] Eddy covariance flux measurements of NO, NO_2, and O_3 were obtained above the mixed deciduous canopy at Harvard Forest in central Massachusetts from April to November 2000. Net deposition of NO_x was observed throughout the measurement period, with average velocity of $\sim$0.2 cm s^{-1}. At night, NO_2 is deposited at a rate that depends nonlinearly on NO_2 concentration and cannot be explained by N_2O_5 hydrolysis, suggesting HONO formation by heterogeneous disproportionation of NO_2. During the day, photochemically driven NO_x fluxes conform to the predicted behavior based on gradients of light and eddy diffusivity through the canopy, with residual net flux attributable to both stomatal and nonstomatal processes. The results were consistent with a compensation point for NO_2 near 1.5 nmol mol^{-1}. These results were confirmed by independent evidence from NO, NO_2, and O_3 profiles acquired at the site over several years. If the rate of NO_x deposition observed at this site in April through November continues during the winter, it would have a larger potential impact on tropospheric chemistry because mixing depths are shallow and chemical NO_x oxidation is slow during winter; the impact at night is important for the same reasons. The results contradict widely used parameterizations of NO_2 deposition that both overestimate stomatal uptake and do not allow for surface uptake when stomates are closed. *INDEX TERMS:* 0315 Atmospheric Composition and Structure: Biosphere/atmosphere interactions; 0322 Atmospheric Composition and Structure: Constituent sources and sinks; 0345 Atmospheric Composition and Structure: Pollution—urban and regional (0305); 0365 Atmospheric Composition and Structure: Troposphere—composition and chemistry; *KEYWORDS:* nitrogen oxides, fluxes, troposphere

Citation: Horii, C. V., J. W. Munger, S. C. Wofsy, M. Zahniser, D. Nelson, and J. B. McManus (2004), Fluxes of nitrogen oxides over a temperate deciduous forest, *J. Geophys. Res.*, *109*, D08305, doi:10.1029/2003JD004326.

1. Introduction

[2] Tropospheric NO_2 is the critical nitrogen oxide radical in the photochemical formation of O_3. The NO_x species, NO and NO_2, rapidly interconvert in fast photochemical reactions (1)–(3). The cycle of reactions (1a), (2), and (3) has no net effect on O_3, but the sequence of reactions (1b), (2), and (3) produces O_3.

$$NO + O_3 \rightarrow NO_2 + O_2 \quad (1a)$$

$$NO + RO_2 \rightarrow NO_2 + RO \quad (1b)$$

$$NO_2 + h\nu \rightarrow NO + O(^3P) \quad (2)$$

$$O(^3P) + O_2 \rightarrow O_3 \quad (3)$$

0148-0227/04/2003JD004326

Production of O_3 is limited by removal of NO_2, either by chemical reactions to make the nonradical species HNO_3, or by deposition to the surface. Chemical removal during the day is mainly due to reaction of NO_2 with OH radicals, while at night removal proceeds via reaction with O_3 to make the nitrate radical (NO_3), which reacts with NO_2 to form N_2O_5 that can hydrolyze to HNO_3. These chain-terminating steps are slow compared to the chain propagating reactions (1)–(3), allowing one molecule of NO_x to be cycled many times before removal. Up to 100 molecules of O_3 may be generated for each NO_x molecule entering the remote troposphere, with $\sim$5 O_3 thought to be typically produced per unit NO_x in the rural eastern United States [*Liu et al.*, 1987; *Hirsch et al.*, 1996].

[3] Deposition of NO_2 to surfaces bypasses atmospheric oxidation to HNO_3 and reduces the amount of NO_x exported to the remote troposphere, thus potentially reducing tropospheric O_3 production even if NO_2 deposition constitutes a small fraction of the total flux of fixed N to the surface [*Jacob et al.*, 1993; *Liang et al.*, 1998]. Chamber studies using NO_2 concentrations between 0.1

and 100 nmol mol^{-1} have reported significant rates for uptake of NO_2 by vegetation through stomates [*Rondón et al.*, 1993; *Thoene et al.*, 1996; *Geßler et al.*, 2000; *Sparks et al.*, 2001], adsorption on foliar surfaces [*Geßler et al.*, 2002], and deposition to forest floors and soils [*Hanson and Lindberg*, 1991; *Eugster and Hesterberg*, 1996]. The NO_2 compensation point, the ambient concentration below which NO_2 is emitted from stomates, has been estimated by linear regression from higher concentrations [*Thoene et al.*, 1996] and observed directly [*Rondón et al.*, 1993; *Geßler et al.*, 2000; *Sparks et al.*, 2001; *Geßler et al.*, 2002] at values between 0.5 and 3 nmol mol^{-1}. Release of NO_2 by vegetation could significantly elevate global O_3 production rates because NO_x concentrations are lower than the inferred compensation point over much of the globe [*Lerdau et al.*, 2000].

[4] NO does not readily combine with atmospheric radicals to make stable nonradicals, and it is not expected to deposit to surfaces in significant amounts, though there is very little experimental confirmation [*Hanson and Lindberg*, 1991; *Wesely and Hicks*, 2000]. NO is emitted from soils, typically at low rates in temperate forests [*Williams et al.*, 1992; *Munger et al.*, 1996]. Nevertheless, rapid photochemical exchange between NO, O_3 and NO_2 make simultaneous quantification of fluxes for these species a requirement for elucidating NO_x deposition rates [*Fitzjarrald and Lenschow*, 1983].

[5] We present here NO and NO_2 eddy covariance fluxes at the Harvard Forest Environmental Measurement Site for spring throughfall, 2000, augmented by 12 years of data at the site for vertical profiles of NO_2 and NO concentrations and eddy covariance fluxes of O_3 and NO_y. The measurements represent the first simultaneous data for fluxes of NO, NO_2, and O_3 above a tall forest canopy with chemically specific eddy covariance instrumentation. The results allow us to critically test current assumptions about deposition and emission fluxes of NO_x at the whole-canopy scale.

2. Methods

[6] We studied a 50- to 70-year-old mixed deciduous forest of red oak and red maple, with scattered hemlock, red and white pine at Harvard Forest in central Massachusetts (42.54N, 72.18W; elevation 340 m). The landscape is ~95% forested and moderately hilly; the distance to the closest paved road is >1.5 km and to the nearest small town >10 km. Two wind directions dominate: northwest flows bring relatively cool, dry, unpolluted air, and southwest winds bring warm, humid, significantly more polluted air [*Moody et al.*, 1998; *Munger et al.*, 1996]. We utilized two towers for this study: a permanent 30-m Rohn 25G tower, used since 1990 to measure eddy fluxes of CO_2, NO_y, and O_3, along with vertical profiles of NO, NO_2, O_3, and other species; and a temporary steel scaffolding tower, 23 m high (just above the top of the canopy), situated about 100 m to the SE and outfitted with a sonic anemometer and a tunable diode laser absorption spectrometer (TDLAS) configured to measure eddy covariance fluxes and concentrations of NO_2 and concentrations of HNO_3 [*Horii*, 2002]. Data from the two towers were matched and averaged into an hourly data set, available at http://www-as.harvard.edu/chemistry/index.html.

2.1. NO_x Photolysis-Chemiluminescence (P-C) Measurements

[7] The P-C system measures NO and NO_2 concentration profiles at heights of 29, 24.1, 18.3, 12.7, 7.5, 4.5, 0.8, and 0.3 m on the permanent tower [*Munger et al.*, 1996]. From late August to mid October 2000, it was reconfigured to measure NO concentrations at 10 Hz at the 29 m sampling height in order to determine eddy covariance fluxes for NO. Calibrations were made using standard gas mixtures for NO and NO_2, traceable to NIST. The NO_2 and NO standards were cross calibrated by titrating the NO standard with O_3 and by analyzing both using the NO_y detector equipped with a hot gold catalyst for reducing NO_y to NO.

2.2. NO_2 TDLAS Measurements

[8] The TDLAS [*Horii et al.*, 1999; *Horii*, 2002] ran two diodes simultaneously from April through November 2000. One channel measured NO_2 concentrations at 1 Hz and the other measured concentrations of HNO_3. The transition line strengths and pressure broadening coefficients used to compute absorption cross sections were obtained from the HITRAN spectral database [*Rothman et al.*, 1998]. TDLAS calibration relied on independent laboratory determination of spectroscopic parameters (light path length, laser mode purity and frequency, laser tuning rate function, and laser line width), which were also checked in the field monthly using standard additions of HNO_3 and NO_2, ambient water vapor, and a Germanium etalon. Multiple levels of cross calibration were maintained throughout the experiment. Independent cross-checks were obtained by comparing concentrations of H_2O inferred using spectral lines in both the NO_2 and HNO_3 spectral ranges (1590 and 1720 cm^{-1}, respectively) with H_2O data from hygrometers on the main tower. One-second, integrated measurements of both zero air and a constant NO_2 permeation tube source show that the RMS noise over a wide range of [NO_2] was 80 pmol mol^{-1}. NO_2 precision does not scale with trace gas concentration in the TDLAS; instead, precision is limited by the background noise of the photovoltaic detectors, the output power of the laser diode, and the finite reflectivity of the multiple pass mirrors. Short- and long-term temperature and pressure instabilities within the instrument limit the improvement of precision obtained from longer integration times to a factor of 2 to 4. Concentrations of NO_2 obtained by TDLAS and P-C instruments were directly compared during 459 hours of concurrent measurements (4 April to 29 August 2000); the orthogonal distance regression of hourly data for the TDLAS versus P-C had a slope of 1.1 ± 0.2 (95% confidence interval, R^2 = 0.91) and an intercept indistinguishable from zero [*Horii*, 2002].

2.3. O_3 UV Absorbance and Chemiluminescence Measurements

[9] O_3 concentration profiles and eddy covariance flux measurements on the main tower employ UV absorbance (Dasibi 1003AH, sampling at the same heights as above) and C_2H_4-chemiluminescence (29 m sampling height), respectively [*Munger et al.*, 1996]. The Dasibi 1003AH was calibrated by comparison to a calibration unit or return

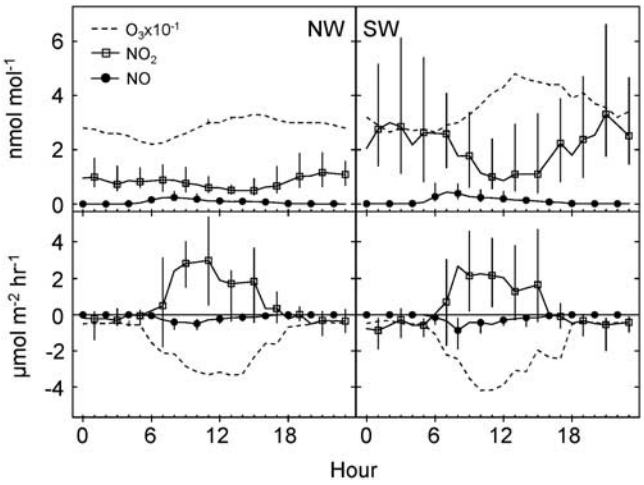

Figure 1. Diel cycles of (top) median concentrations and (bottom) fluxes for the (left) northwest (270°–45°) and (right) southwest (180°–270°) wind sectors at Harvard Forest, April–November 2000, for NO_2 at 22 m (squares), NO at 29 m (circles), and $O_3 \times 10^{-1}$ at 29 m (dashed line, shown for reference). For NO and NO_2, symbols are plotted at even and odd hours, respectively (lines go through hourly points), and vertical bars indicate 25th and 75th percentiles.

to the factory, and the C_2H_4-chemiluminescence instrument calibration was checked by routine comparison to the Dasibi 1003AH.

2.4. Micrometeorology and Auxiliary Measurements

[10] Triaxial sonic anemometers were oriented westward at the eddy covariance sampling height on each tower; data for vertical and horizontal wind velocities and virtual temperatures were acquired at 10 Hz to compute eddy covariance fluxes of heat, momentum, NO, and NO_2, and at 5 Hz for O_3 [*Munger et al.*, 1996, 1998]. Photosynthetic photon flux density (PPFD, 400–700 nm) was measured continuously at 29 m on the main tower using a LI-COR quantum sensor.

2.5. Eddy Covariance Fluxes

[11] We computed 30-min mean fluxes of trace gases from the covariance of linearly detrended time series for vertical velocity (w') and trace gas concentrations (C'). To correct for relatively slow instrument response times, data for virtual temperature and w were processed using instantaneous measurements by the sonic anemometer, then repeated using a set of single-pole low-pass numerical filters matched with the time response of each gas sensor. The ratio of the "filtered" heat flux for each 30-min interval to the unfiltered heat flux provided an estimate of flux lost by instrumental smoothing of high-frequency fluctuations [*Goulden et al.*, 1996; *Munger et al.*, 1996, 1998]. Corrections were typically 20% or smaller for all chemical species.

3. Results and Discussion

[12] Figure 1 shows median values at each hour of the day for NO, NO_2, and O_3 concentrations (top panels) and fluxes (bottom panels) for April through November 2000, segregated by wind sector. Photochemical production of NO during the day and conversion to NO_2 at night are apparent (top panels). Concentrations of O_3 are typically much greater than NO_x, thus chemical reactions do not significantly perturb the vertical O_3 gradients and fluxes set by mixing and surface deposition [*Munger et al.*, 1996].

3.1. Nighttime Fluxes

[13] We observed downward fluxes of NO_2 during all measurement seasons in 2000 (spring, summer, and fall) at night, for both clean (NW) and polluted (SW) wind sectors (Figure 1, bottom panels). Drainage flows at the surface in stable nighttime conditions make it difficult to quantify ecosystem exchange of respired CO_2 at night by eddy covariance [*Staebler and Fitzjarrald*, 2004]. However, the small turbulent fluxes of depositing species observed by eddy covariance are likely an accurate measure of their vertical exchange. When momentum is not being transported downward, neither are scalars.

[14] The downward nighttime NO_2 flux increases with NO_2 concentration (Figure 2). The polynomial regression function $FNO_2 = V_0[NO_2] + a[NO_2]^2$ applied to hourly nighttime data yields $R^2 = 0.60$, $V_0 = -0.08 \pm 0.03$ ($p = 0.01$), and $a = -0.013 \pm 0.001$ ($p < 0.0001$). The quadratic dependence in the regression is largely driven by the two nights during the sampling period when the median concentration of NO_2 exceeded 10 nmol mol^{-1}. Excluding these nights, neither the overall fit nor the coefficient a is statistically significant. However, even for concentrations below 10 nmol mol^{-1}, the coefficient V_0 is negative and significant ($V_0 = -0.16 \pm 0.06$, $p = 0.005$). The regression suggests that the nighttime deposition velocity of NO_2 ($V_d(NO_2) = -FNO_2/[NO_2]$) increases from approximately

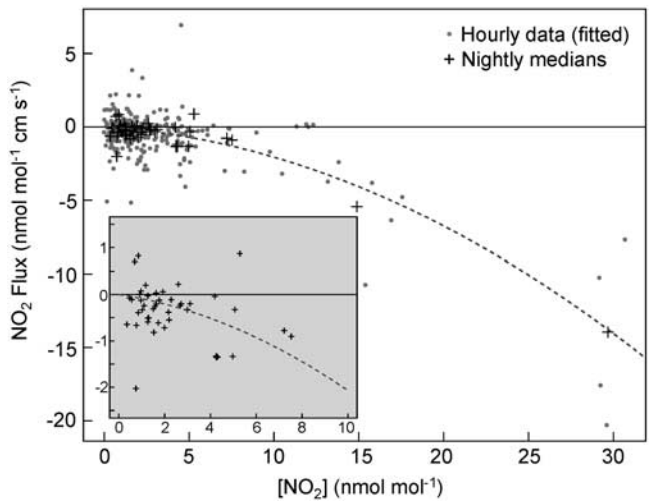

Figure 2. Nighttime hourly (dots) and median nightly (pluses) NO_2 flux versus concentration. The curve represents the function $FNO_2 = F_0 + V_0\,[NO_2] + a\,[NO_2]^2$, with coefficients derived from a least squares fit to the hourly data. The flux is expressed in units of concentration times velocity (nmol mol^{-1} cm s^{-1}) in order to simplify the interpretation of the coefficients in the least squares fit. Pressure and temperature corrections have been taken into account in the conversion from density to mixing ratio flux units. The inset shows an expansion of both x and y axes with nightly medians only. See color version of this figure in the HTML.

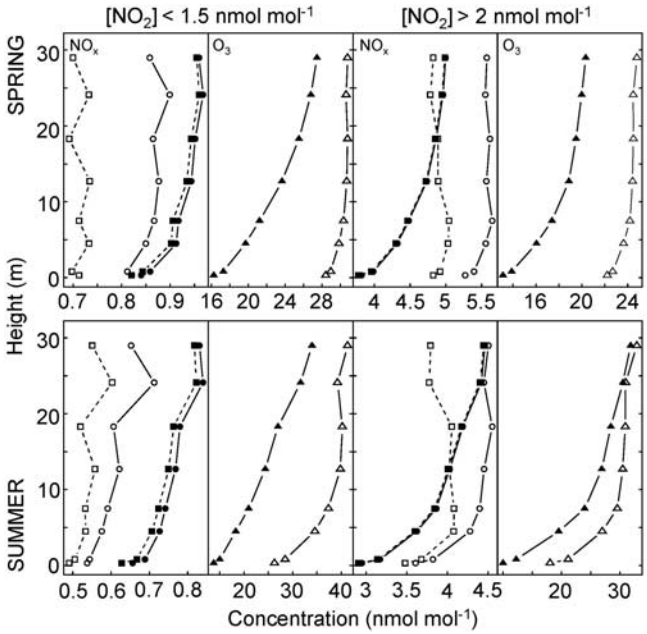

Figure 3. Mean vertical profiles of NO_2 (squares, dashed lines), NO_x = NO_2 + NO (circles, solid lines), and O_3 (triangles, solid lines) during the day (open symbols) and night (solid symbols) on the main Harvard Forest tower in 2000. (top) April and May data. (bottom) Data from June, July, and August. (September–November profiles are unavailable for this year.) (left) Limited to $[NO_2] < 1.5$ nmol mol^{-1}. (right) Limited to $[NO_2] > 2$ nmol mol^{-1}. Note the clear influence of forest canopy development from spring to summer on the NO_2 profile at higher $[NO_2]$ and the masking of this effect at low $[NO_2]$ by apparent canopy-level NO_2 emission. The year 2000 profiles are representative of those observed between 1990 and 2002.

0.2 cm s^{-1} at $[NO_2]$ = 1 nmol mol^{-1} to 0.5 cm s^{-1} at $[NO_2]$ = 30 nmol mol^{-1}. This NO_2 deposition is equal to 6–20% of nighttime NO_y flux observed by eddy covariance at the site [*Horii*, 2002].

[15] The nighttime deposition of NO_2 in the canopy is confirmed by observations of NO, NO_2, and O_3 concentration profiles at the main tower (Figure 3). Concentrations of NO above the canopy at night are very small, often below the instrumental detection limit and indistinguishable from zero. Nighttime $[NO_x]$ profiles exhibit a deposition signature similar to O_3, with dC/dz > 0, notwithstanding the small soil emissions of NO at the site of $\leq$0.9 μmol m^{-2} h^{-1} [*Munger et al.*, 1996]. We compared the NO_x and O_3 fluxes by inferring average eddy diffusivity, K, derived from the flux-gradient relationship for each species: $F = -K\, dC/dz$, using the measured eddy covariance fluxes of NO_2 and O_3 above the canopy and the average concentration gradient between 5 m and 24 m. We found nighttime values of K $\approx$ 2400 cm^2 s^{-1} with remarkable consistency: K_{NO_x}/K_{O_3} varied between 0.5 and 1.5 with a mean value ~1 independent of season (April–August) and NO_x concentration.

[16] Evidence for deposition to surfaces such as leaves, litter, bark, and soil has been reported previously by *Eugster and Hesterberg* [1996] and *Hanson and Lindberg* [1991, and references therein]. Hydrolysis of N_2O_5 on forest surfaces below the sensor height is a possible mechanism (reactions (4)–(6)). The rate-limiting step is formation of NO_3 in reaction (4) [e.g., *Jacob*, 2000]:

$$NO_2 + O_3 \rightarrow NO_3 + O_2 \quad (4)$$

$$NO_3 + NO_2 + M \rightarrow N_2O_5 + M \quad (5)$$

$$N_2O_5 + H_2O \rightarrow 2HNO_3. \quad (6)$$

We estimated an upper limit for NO_2 deposition due to this process by calculating production of NO_3 in reaction (4) from data for O_3 and NO_2 (Figure 3) and assuming 100% efficiency for reactions (5) and (6) and concluded that hydrolysis of N_2O_5 accounts for at most a minor fraction (<30%) of the observed nighttime NO_2 deposition at all observed concentrations.

[17] Nighttime deposition of NO_2 (and the possible nonlinear dependence of flux on concentration) could also be explained by heterogeneous conversion to HONO and HNO_3, as observed on aerosols [*Notholt et al.*, 1992]. The mechanisms and kinetics of the associated NO_2 reactions on hydrated surfaces are not fully understood. Heterogeneous NO_2 hydrolysis likely proceeds by the overall reaction

$$2NO_2(g) + H_2O(a) \rightarrow HONO(g) + HNO_3(a) \quad (7)$$

[*Goodman et al.*, 1999]. Laboratory studies have shown first-order kinetics in NO_2 for reaction (7) at μmol mol^{-1} (parts per million) concentrations, with NO_2 adsorption as the rate-limiting step, but the rate at low concentrations on forest surfaces is unknown. The atmospheric mechanism is likely to involve formation of N_2O_4 as an intermediate on the surface [*Finlayson-Pitts et al.*, 2003]. As in the N_2O_5 hydrolysis mechanism, the aqueous phase HNO_3 produced in reaction (7) is not likely to be released to the gas phase, but HONO might be returned to the atmosphere.

[18] *Harrison et al.* [1996] observed upward HONO fluxes over vegetated surfaces at NO_2 concentrations above 10 nmol mol^{-1}, with a quadratic dependence of [HONO] on $[NO_2]$; likewise, HONO measurements by *Thornberry et al.* [2001] are consistent with heterogeneous production from NO_2. If the observed NO_2 flux at Harvard Forest is the result of reaction (7), then approximately half could return to the atmosphere as gas phase HONO. Since HONO is rapidly photolyzed to NO and OH upon sunrise, up to half of the nighttime NO_2 deposition would therefore not contribute to daily net loss of NO_x from the atmosphere. The possible heterogeneous HONO formation at the surface during the night is important to daytime HO_x chemistry, delivering a burst of OH and NO radicals to the surface layer at sunrise when HONO photolyzes.

3.2. Daytime Fluxes

[19] During daylight hours we observed large compensating fluxes, upward for NO_2 and downward for NO (Figure 1); these are largely due to the influence of the forest canopy on the vertical NO_2 photolysis gradient (reaction (3)) [*Gao et al.*, 1993]. Higher irradiance above the canopy favors production of NO (reaction (2)); lower light below

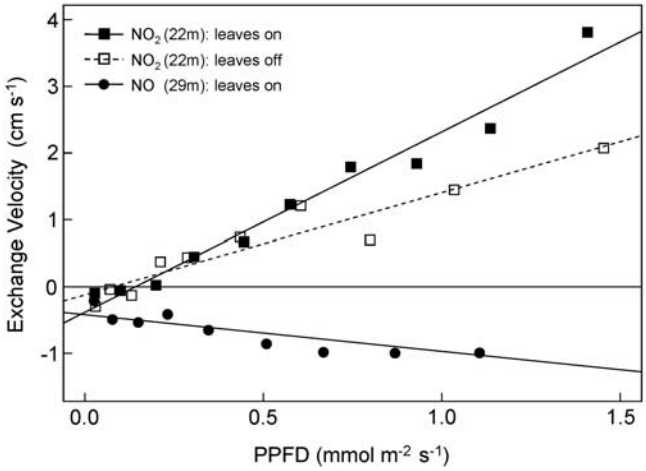

Figure 4. Daytime emission velocities of NO_2 (squares) and NO (circles) versus photosynthetic photon flux density (PPFD). Symbols are medians of hourly data binned by percentiles of above-canopy PPFD. NO_2 flux data are segregated into full-canopy conditions from early June to mid October (solid symbols), and leafless periods in April–May and October–November (open symbols). Linear fits to binned median points are VNO_2 (leaves on) = $(-0.4 \pm 0.1) + (2.7 \pm 0.2)$ PPFD, $R^2 = 0.97$; VNO_2 (leaves off) = $(0.1 \pm 0.1) + (1.5 \pm 0.2)$ PPFD, $R^2 = 0.90$; VNO (leaves on) = $(-0.42 \pm 0.07) + (-0.5 \pm 0.1)$ PPFD, $R^2 = 0.78$. Midsummer leaf area index at Harvard Forest is ~3.4, whereas the area index for bare stems and twigs is only 0.9 (Harvard Forest Online Data Archive, available at http://www-as.harvard.edu/chemistry/index.html).

the canopy shifts the balance toward NO_2 (reactions (1a) and (1b)). The magnitude of the daytime upward flux of NO_2 in Figure 1 is greater than the corresponding downward flux of NO, an artifact of the different sampling heights for NO (29 m on the main tower) and the TDLAS NO_2 (22 m on the auxiliary tower). *Gao et al.* [1993] showed in a modeling study that the fluxes of NO and NO_2 just above the canopy should be very sensitive to height.

[20] The eddy covariance fluxes of NO and NO_2 are correlated on an hourly basis during the daytime: An orthogonal distance fit yields $FNO_2 = -(4.0 \pm 0.1)FNO$, $R^2 = 0.80$. The exchange velocities for NO and NO_2 follow light levels as measured by PPFD (Figure 4), as expected for vertical gradients associated with photolysis (Figure 3). There is a seasonal change in the dependence of daytime NO_2 flux on PPFD, correlated with canopy development, with a lower slope of the NO_2 exchange velocity versus PPFD for leafless periods. This result is also consistent with the expected effect of a smaller above- to below-canopy light gradient under leafless conditions, although it does not rule out a chemical or biological role in NO_2 exchange for the leaves. Since PPFD is a commonly measured and modeled quantity, we make use of this quantity as a proxy for photochemical activity in a simple parameterization of NO_x flux at our site.

3.3. Parameterization of NO_x Fluxes

[21] Global 2-D and 3-D models often parameterize NO_2 flux using canopy resistances assumed similar to O_3 [e.g., *Wang et al.*, 1998; *Wesely and Hicks*, 2000]. Although leaf-level measurements indicate a high degree of stomatal control over NO_2 flux similar to the stomatal uptake of O_3, the dearth of canopy-level NO_2 flux measurements calls this assumption into question. Recent results also raise doubts about the dominance of stomatal control of O_3 deposition to a forest canopy in the presence of biogenic hydrocarbons [*Kurpius and Goldstein*, 2003]. We therefore seek to assess the processes responsible for the observed NO_x surface fluxes independent of assumptions of similarity to O_3. In the following parameterization, we adopt the hypothesis that photochemical NO-NO_2 cycling via reactions (1)–(3) arising from canopy-induced light gradients has no effect on net deposition and represent it in our data set by a simple light-dependent term. We then use a multiple regression to determine the most likely contributions of other processes to the net flux.

[22] We represent fluxes of NO_2 by the sum of the following terms: $V_0 \cdot [NO_2]$, a constant exchange velocity term; $a \cdot [NO_2]^2$, a concentration-dependent exchange velocity term; $(b + f) \cdot \mathrm{PPFD} \cdot [NO_2]$, a light-dependent photochemical cycling term allowing for differences between full-canopy and leafless conditions; and $\gamma \cdot g_c$, a term representing exchange processes under stomatal control. Stomatal conductance (g_c) (calculated using the measured water vapor flux and the Penman-Monteith equation after *Shuttleworth et al.* [1984]) correlates with PPFD, but the diel variations of the two differ in terms of morning/afternoon asymmetry and at dawn and dusk, making it possible to distinguish stomatally controlled from simple light-dependent processes, if both are strong enough. Thus we parameterize the flux of NO_2, 2 m above the canopy, day and night, by the function

$$FNO_2 = V_0 \cdot [NO_2] + a \cdot [NO_2]^2 + (b + f) \cdot \mathrm{PPFD} \cdot [NO_2] + \gamma \cdot g_c \quad (8)$$

where f is added to the coefficient of PPFD to account for the observed difference between full-canopy and leaves-off conditions. The regression was run to determine the coefficients V_0, a, b, and f using observed FNO_2 and $[NO_2]$ on the full data set as well as various subsets of data, including high-NO_2, low-NO_2, daytime, and nighttime conditions (Table 1). The values of the coefficients are consistent whether they are computed from the full data set or the selected subsets. However, for low-NO_2 conditions some coefficients have low statistical significance. The coefficient of the stomatal term, γ, is significant in most of the fits and follows the expected behavior for a stomatal process with a compensation point. The $\gamma \cdot g_c$ term appears to contribute a downward component of NO_2 flux when NO_2 is high (>2 nmol mol^{-1}) and an upward flux when NO_2 is low (<1.5 nmol mol^{-1}). Low-NO_x conditions dominate at the site [*Munger et al.*, 1996].

[23] Fluxes of NO from soils at our site are measurable but small. The major contributor to FNO during the day is the simple dependence on PPFD. We include a constant exchange velocity term ($V_{0\_NO} \cdot [NO]$) and a light-dependent term ($b' \cdot \mathrm{PPFD} \cdot [NO]$), giving the NO flux 7 m above the canopy as

$$FNO = V_{0\_NO} \cdot [NO] + b' \cdot \mathrm{PPFD} \cdot [NO]. \quad (9)$$

Table 1. Multifactor Regressions of NO_2 and NO Flux Data Using All Available Hourly Observations of $[NO_2]$, PPFD, FNO_2, and FNO and Calculated Stomatal Conductance, g_c, at Harvard Forest, April–November 2000[a]

	All Data (R^2 = 0.60, N = 928)	$[NO_2]$ < 1.5, nmol mol^{-1} (R^2 = 0.15, N = 464)	$[NO_2]$ > 2, nmol mol^{-1} (R^2 = 0.75, N = 306)	Day Only (R^2 = 0.63, N = 412)	Night Only (R^2 = 0.60, N = 316)
V_0	−0.14 ± 0.03	*−0.3 ± 0.4*	−0.12 ± 0.04	−0.39 ± 0.09	−0.08 ± 0.03
a	−0.009 ± 0.002	*0.2 ± 0.3*	−0.010 ± 0.002	*0.008 ± 0.009*	−0.013 ± 0.001
b	2.23 ± 0.07	1.7 ± 0.4	2.4 ± 0.1	2.3 ± 0.1	NA
f	−1.32 ± 0.09	−1.2 ± 0.5	−1.4 ± 0.1	−1.3 ± 0.1	NA
γ	*0.2 ± 0.2*	0.8 ± 0.4	−1.6 ± 0.8	0.5 ± 0.3	NA

[a]For z = 22 m: $FNO_2 = V_0 \cdot [NO_2] + a \cdot [NO_2]^2 + (b + f) \cdot PPFD \cdot [NO_2] + \gamma \cdot g_c$. Day-only and night-only regressions exclude dawn and dusk. Note the overall consistency of direction and magnitude of statistically significant terms, with the exception of the coefficient of g_c, which changes sign between high- and low-NO_2 conditions. Terms with p > 0.1 are italicized. For each term, units are as follows: V_0, cm s^{-1}; a, (nmol mol^{-1})$^{-1}$ cm s^{-1}; b, cm s^{-1} (μmol m^{-2} s^{-1})$^{-1}$; f, cm s^{-1} (μmol m^{-2} s^{-1})$^{-1}$, where $f = 0$ for leaves-on conditions; and γ, nmol mol^{-1}.

The resulting parameterization indicates a small deposition velocity, with large fluxes due to photochemical cycling, using all available data (956 hours), $R^2 = 0.92$, $V_{0\_NO} = -0.25 \pm 0.02$ cm s^{-1}, and $b' = -0.87 \pm 0.03$ cm s^{-1} (μmol m^{-2} s^{-1})$^{-1}$.

3.4. Analysis of Net NO_x Flux

[24] Because net NO flux (soils and deposition) appears small, and the purely gas phase photochemical contributions to NO and NO_2 fluxes arising from canopy light gradients should cancel when considering net ecosystem flux, we estimate the net flux of NO_x from the FNO_2 parameterization (8) by omitting the photochemical cycling components:

$$FNO_x(\text{net}) \approx FNO_2 - (b+f) \cdot PPFD \cdot [NO_2] = V_0 \cdot [NO_2] + a \cdot [NO_2]^2 + \gamma \cdot g_c. \quad (10)$$

Figure 5 illustrates the relative contributions of each term to net flux and the resulting net NO_2 exchange velocity, for all conditions and for high-NO_2 periods, using the coefficients from Table 1, measured NO_2 concentrations, and calculated g_c.

[25] When NO_2 concentrations are low during the day, some NO_2 is emitted under stomatal control but is offset by NO_2 deposition to other surfaces. When NO_2 concentrations are high during the day, NO_2 is deposited under stomatal control, as much as doubling the rate of NO_2 deposition. For most conditions at Harvard Forest, nonstomatal deposition accounts for the largest fraction of the flux, during the night as well as the day. *Lerdau et al.* [2000] noted that leaf-level observations of NO_2 emission at low ambient concentrations were inconsistent with current understanding of NO_x chemistry and observations in the remote troposphere. The overwhelming impact of nonstomatal deposition at the canopy level appears to provide a resolution to this conundrum.

[26] At Harvard Forest the daytime net NO_x flux was ~2% of total daytime NO_y deposition during the summer [*Horii*, 2002]. The lifetime of NO_x associated with deposition, on the basis of an average net NO_x deposition velocity of 0.2 cm s^{-1} and regionally representative mixed layer depths [*Holzworth*, 1967], varies between 10 days in summer and 4 days in winter, assuming surface deposition continues throughout the year as it does from early spring through late fall. This lifetime may decrease to less than 24 hours during shallow nighttime inversions. In comparison, the characteristic time for NO_2 oxidation by OH varies from less than 12 hours in summer to more than 5 days in winter [*Munger et al.*, 1998]. Evidently, direct NO_x deposition to forest surfaces has the largest impact on tropospheric chemistry when mixing layer depths are shallow and when other oxidative processes are relatively slow.

[27] The daytime NO_x and O_3 profiles for April–August 2000 (Figure 3) are qualitatively consistent with the independent eddy covariance flux measurements and net NO_x flux analysis. Under low-NO_x conditions, profiles have a weak gradient, implying a net NO_x flux approaching zero, with nonstomatal deposition to the ground offset by apparent emission in the upper canopy; the persistent NO_x enhancement at 24 m may correspond to stomatal or other UV-induced NO_2 emission reported from vegetation at ambient concentrations below 1 nmol mol^{-1} [*Hari et al.*,

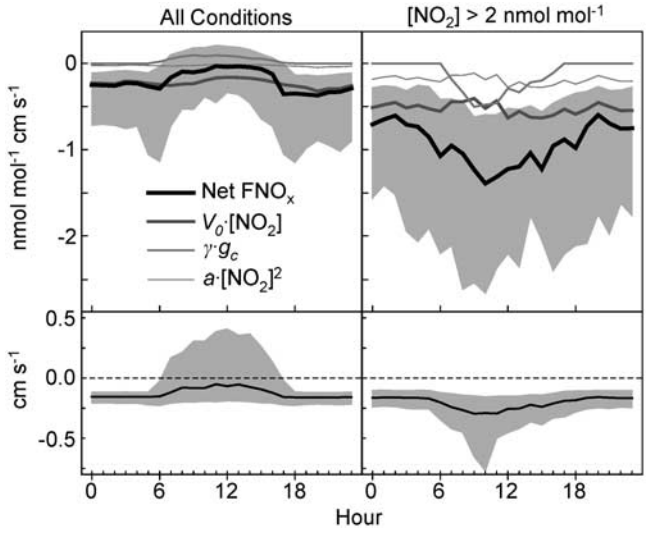

Figure 5. (top) Individual contributing terms (colored lines) and the net NO_2 flux (black line) based on the coefficients in Table 1, measured $[NO_2]$, and calculated g_c. The shaded regions indicate reasonable bounds on the net flux: The upper bound is the 75th percentile of net FNO_2 calculated using the upper confidence limit of the coefficients; the lower bound is the 25th percentile calculated with the lower confidence limit of the coefficients. (bottom) Net NO_x deposition velocity with upper and lower bounds calculated as in the top panels. Panels on the left use all data and the corresponding coefficients from Table 1. Panels on the right use data hours when NO_2 > 2 nmol mol^{-1} and high-NO_2 coefficients. See color version of this figure in the HTML.

2003]. The profiles indicate that net NO_x deposition is stronger at higher [NO_x] compared to lower [NO_x], and during the summer compared to the early spring. As discussed earlier, the nighttime profiles in Figure 3 also support the results of the net NO_x flux analysis showing deposition during nondaylight hours.

4. Conclusion

[28] On the basis of both flux data and vertical profiles, we find that nighttime NO_2 flux at Harvard Forest is predominantly downward, including clean air conditions. The results contradict widely used parameterizations of NO_2 deposition (e.g., big-leaf, resistance-in-series models, following the *Wesely* [1989] scheme) that do not provide for surface uptake when stomates are closed. Because N_2O_5 hydrolysis is insufficient to account for the observed deposition flux (particularly at the highest NO_2 concentrations observed), HONO production may be important. Daytime fluxes of NO and NO_2 are strongly coupled and dominated by simple photochemical exchange that does not contribute to net NO_x flux. We conclude that NO_2 and NO fluxes can be parameterized in terms of known physical processes to derive a deposition velocity for NO_2 of $\sim$0.2 cm s^{-1}. Stomatal influence is weaker than typically assumed in models, and it changes sign depending on NO_2 concentrations, with overall near zero deposition or emission in the daytime for NO_x less than $\sim$1.5 nmol mol^{-1}, and significant stomatal uptake for high NO_x. These results identify a canopy scale deposition process that is not apparent in leaf-level measurements. They highlight the importance of including both nonstomatal deposition and a compensation point in NO_2 surface exchange parameterizations embedded in models of tropospheric chemistry and transport. Overall, we have found by direct measurements in field conditions that vegetation serves as a net sink for NO_x radicals, with the sink strength increasing as NO_x concentration rises. Contrary to previous assumptions, the sink persists at night and in the early spring and late fall dormant seasons. The persistent deposition due to nonstomatal processes provides a potential resolution to the problem that extensive NO_2 emission from foliage where NO_2 is below the compensation point would be inconsistent with our understanding of NO_x chemistry and with observations in the remote troposphere.

[29] **Acknowledgments.** This work was supported by NASA Headquarters under the Earth System Science Fellowship grant NGT5-30205, by the NOAA Global Change Program grant NA46GP0119, by the National Science Foundation grant ATM-9981282, and by the Office of Science, Biological and Environmental Research Program (BER), U.S. Department of Energy, through the Northeast Regional Center of the National Institute for Global Environmental Change (NIGEC) under the Cooperative Agreement DE-FC02-03ER6313. The authors gratefully acknowledge the assistance of Aerodyne Research staff members Jeff Mulholland and Bob Prescott and Harvard University engineers Alfram Bright and Bruce Daube for their work on the TDLAS instrument and thank John Budney, Elaine Gottleib, Jack Edwards, Edythe Ellin, Don Hesselton, Felicia Frizzell, and Shane Heath for their support at the HFEMS.

References

Eugster, W., and R. Hesterberg (1996), Transfer resistances of NO_2 determined from eddy correlation flux measurements over a litter meadow at a rural site on the Swiss plateau, *Atmos. Environ.*, *30*, 1247–1254.

Finlayson-Pitts, B. J., L. M. Wingen, A. L. Sumner, D. Syomin, and K. A. Ramazan (2003), The heterogeneous hydrolysis of NO_2 in laboratory systems and in outdoor and indoor atmospheres: An integrated mechanism, *Phys. Chem. Chem. Phys.*, *5*, 223–242.

Fitzjarrald, D. R., and D. H. Lenschow (1983), Mean concentration and flux profiles for chemically reactive species in the atmospheric surface layer, *Atmos. Environ.*, *17*, 2505–2512.

Gao, W., M. L. Wesely, and P. V. Doskey (1993), Numerical modeling of the turbulent diffusion and chemistry of NO_x, O_3, isoprene, and other reactive trace gases in and above a forest canopy, *J. Geophys. Res.*, *98*, 18,339–18,353.

Geßler, A., M. Rienks, and H. Rennenberg (2000), NH_3 and NO_2 fluxes between beech trees and the atmosphere—Correlation with climatic and physiological parameters, *New Phytol.*, *147*, 539–560.

Geßler, A., M. Rienks, and H. Rennenberg (2002), Stomatal uptake and cuticular adsorption contribute to dry deposition of NH_3 and NO_2 to needles of adult spruce (*Picea abies*) trees, *New Phytol.*, *156*, 179–194.

Goodman, A. L., G. M. Underwood, and V. H. Grassian (1999), Heterogeneous reaction of NO_2: Characterization of gas-phase and adsorbed products from the reaction, $2NO_2(g) + H_2O(a) \rightarrow HONO(g) + HNO_3(a)$ on hydrated silica particles, *J. Phys. Chem. A*, *103*, 7217–7223.

Goulden, M. L., J. W. Munger, S.-M. Fan, B. C. Daube, and S. C. Wofsy (1996), Measurements of carbon sequestration by long-term eddy covariance: Methods and a critical evaluation of accuracy, *Global Change Biol.*, *2*, 169–182.

Hanson, P., and S. E. Lindberg (1991), Dry deposition of reactive nitrogen compounds: A review of leaf, canopy, and non-foliar measurements, *Atmos. Environ., Part A*, *25*, 1615–1634.

Hari, P., M. Raivonen, T. Vesala, J. W. Munger, K. Pilegaard, and M. Kulmala (2003), Ultraviolet light and leaf emission of NO_x, *Nature*, *422*, 134.

Harrison, R. M., J. D. Peak, and G. M. Collins (1996), Tropospheric cycle of nitrous acid, *J. Geophys. Res.*, *101*, 14,429–14,439.

Hirsch, A. I., J. W. Munger, D. J. Jacob, L. W. Horowitz, and A. H. Goldstein (1996), Seasonal variation of the ozone production efficiency per unit NO_x at Harvard Forest, Massachusetts, *J. Geophys. Res.*, *101*, 12,659–12,666.

Holzworth, G. C. (1967), Mixing depths, wind speeds and air pollution potential for selected locations in the United States, *J. Appl. Meteorol.*, *6*, 1039–1044.

Horii, C. V. (2002), Tropospheric reactive nitrogen speciation, deposition, and chemistry at Harvard Forest, Ph.D. thesis, Harvard Univ., Cambridge, Mass.

Horii, C. V., M. S. Zahniser, D. D. Nelson, J. B. McManus, and S. C. Wofsy (1999), Nitric acid and nitrogen dioxide flux measurements: A new application of tunable diode laser absorption spectroscopy, *Proc. SPIE Int. Soc. Opt. Eng.*, *3758*, 152–161.

Jacob, D. J. (2000), Heterogeneous chemistry and tropospheric ozone, *Atmos. Environ.*, *34*, 2131–2159.

Jacob, D. J., J. A. Logan, G. M. Gardner, R. M. Yevich, C. M. Spivakovsky, and S. C. Wofsy (1993), Factors regulating ozone export over the United States and its export to the global atmosphere, *J. Geophys. Res.*, *98*, 14,817–14,826.

Kurpius, M. R., and A. H. Goldstein (2003), Gas-phase chemistry dominates O_3 loss to a forest, implying a source of aerosols and hydroxyl radicals to the atmosphere, *Geophys. Res. Lett.*, *30*(7), 1371, doi:10.1029/2002GL016785.

Lerdau, M. T., J. W. Munger, and D. J. Jacob (2000), The NO_2 flux conumdrum, *Science*, *289*, 2291–2293.

Liang, J., L. W. Horowitz, D. J. Jacob, Y. Wang, A. M. Fiore, J. A. Logan, G. M. Gardner, and J. W. Munger (1998), Seasonal budgets of reactive nitrogen species and ozone over the United States, and export fluxes to the global atmosphere, *J. Geophys. Res.*, *103*, 13,435–13,450.

Liu, S. C., M. Trainer, F. C. Fehsenfeld, D. D. Parrish, E. J. Williams, D. W. Fahey, G. Hübler, and P. C. Murphy (1987), Ozone production in the rural troposphere and the implications for regional and global ozone distributions, *J. Geophys. Res.*, *92*, 4191–4207.

Moody, J. L., J. W. Munger, A. H. Goldstein, D. J. Jacob, and S. C. Wofsy (1998), Harvard Forest regional-scale air mass composition by Patterns in Atmospheric Transport History (PATH), *J. Geophys. Res.*, *103*, 13,181–13,194.

Munger, J. W., S. C. Wofsy, P. S. Bakwin, S.-M. Fan, M. L. Goulden, B. C. Daube, and A. H. Goldstein (1996), Atmospheric deposition of reactive nitrogen oxides and ozone in a temperate deciduous forest and a subarctic woodland: 1. Measurements and mechanisms, *J. Geophys. Res.*, *101*, 12,639–12,657.

Munger, J. W., S.-M. Fan, P. S. Bakwin, M. L. Goulden, A. H. Goldstein, A. S. Colman, and S. C. Wofsy (1998), Regional budgets for nitrogen oxides from continental sources: Variations of rates for oxidation and deposition with season and distance from source regions, *J. Geophys. Res.*, *103*, 8355–8368.

Notholt, J., J. Hjorth, and F. Raes (1992), Formation of HNO_2 on aerosol surfaces during foggy periods in the presence of NO and NO_2, *Atmos. Environ. Part A*, *26*, 211–217.

Rondón, A., C. Johansson, and L. Granat (1993), Dry deposition of nitrogen dioxide and ozone to coniferous forests, *J. Geophys. Res.*, *98*, 5159–5172.

Rothman, L. S., et al. (1998), The HITRAN molecular spectroscopic database and HAWKS (HITRAN Atmospheric Workstation): 1996 edition, *J. Quant. Spectrosc. Radiat. Transfer*, *60*, 665–710.

Shuttleworth, W. J., et al. (1984), Eddy correlation measurements of energy partition for Amazonian forest, *Q. J. R. Meteorol. Soc.*, *110*, 1143–1162.

Sparks, J. P., R. K. Monson, K. L. Sparks, and M. Lerdau (2001), Leaf uptake of nitrogen dioxide (NO_2) in a tropical wet forest: Implications for tropospheric chemistry, *Oecologia*, *127*, 214–221.

Staebler, R. M., and D. R. Fitzjarrald (2004), Observing subcanopy CO_2 advection, *Agric. For. Meteorol.*, *122*(3–4), 139–156.

Thoene, B., H. Rennenbert, and P. Weber (1996), Absorption of atmospheric NO_2 by spruce (Picea abies) trees II. Parameterization of NO_2 fluxes by controlled dynamic chamber experiments, *New Phytol.*, *134*, 257–266.

Thornberry, T., et al. (2001), Observations of reactive oxidized nitrogen and speciation of NO_y during the PROPHET summer 1998 intensive, *J. Geophys. Res.*, *106*, 24,359–24,386.

Wang, Y., D. J. Jacob, and J. A. Logan (1998), Global simulation of tropospheric O_3-NO_x-hydrocarbon chemistry: 1. Model formulation, *J. Geophys. Res.*, *103*, 10,713–10,726.

Wesely, M. L. (1989), Parameterization of surface resistances to gaseous dry deposition in regional-scale numerical models, *Atmos. Environ.*, *23*, 1293–1304.

Wesely, M. L., and B. B. Hicks (2000), A review of the current status of knowledge on dry deposition, *Atmos. Environ.*, *34*, 2261–2282.

Williams, E. J., G. L. Hutchinson, and F. C. Fehsenfeld (1992), NO_x and N_2O emissions from soil, *Global Biogeochem. Cycles*, *6*, 351–388.

C. V. Horii, J. W. Munger, and S. C. Wofsy, Division of Engineering and Applied Sciences and Department of Earth and Planetary Science, Harvard University, 20 Oxford Street, Cambridge, MA 02138, USA. (cvolpe@fas.harvard.edu)

J. B. McManus, D. Nelson, and M. Zahniser, Aerodyne Research, Inc., 45 Manning Road, Billerica, MA 01821, USA.